Catalysis Science & Technology

rsc.li/catalysis

ROYAL SOCIETY OF CHEMISTRY | Celebrating IYPT 2019

COMMUNICATION
Hanna Härelind *et al.*
Direct observation of atomically-resolved silver species on a silver alumina catalyst active for selective catalytic reduction of nitrogen oxides

COMMUNICATION

Check for updates

Direct observation of atomically-resolved silver species on a silver alumina catalyst active for selective catalytic reduction of nitrogen oxides

Hannes Kannisto,[a] Magnus Skoglundh, [ID][a] Kalle Arve,[b]
Eva Olsson[c] and Hanna Härelind [ID] *[a]

We characterize the size and state of the silver species in a 2 wt% silver alumina catalyst, which is highly active for the selective catalytic reduction of nitrogen oxides with ammonia or hydrocarbons as reductant. The silver alumina catalyst is prepared by a single-step sol–gel method and characterized with X-ray photoelectron and ultraviolet-visible spectroscopy, and high-resolution transmission electron microscopy. We show, for the first time, direct observations of atomically-resolved silver species and silver clusters on the silver alumina catalyst. The results determine the existence of these silver species on the alumina support, which corroborate previously reported indirect observations, and strengthen the hypothesis of small silver clusters as active sites for the selective catalytic reduction of nitrogen oxides.

Silver alumina (Ag/Al_2O_3) is a promising catalyst for the selective catalytic reduction of nitrogen oxides (SCR) in net-oxidizing environments, such as the exhausts from lean-burn or diesel engines, where the conventional three-way catalyst lacks in performance. A reducing agent, such as ammonia derived from urea or hydrocarbons provided by the fuel, is injected before the SCR catalyst, where it reacts with the nitrogen oxides (NO_x) forming less harmful products like molecular nitrogen, water and carbon dioxide.[1] The Ag/Al_2O_3 catalyst was first shown to be active for SCR with propane as reductant by Miyadera[2] and has later been shown to be active for SCR with various types of hydrocarbons (HC-SCR)[1,3–9] and recently with a combination of ethanol and ammonia.[10] Since the work of Satokawa,[11] reporting that the addition of small amounts of hydrogen promotes the activity for HC-SCR over

this system, several reports on the role of hydrogen have been published[1,12–16] (and references herein). The active site for the HC-SCR reaction over Ag/Al_2O_3 has been suggested to be partially charged silver clusters of about 3–4 silver atoms in size.[12,17–19] This suggestion is experimentally supported by *in situ* ultraviolet-visible (UV-vis)[18,19] and *in situ* extended X-ray absorption fine structure (EXAFS)[17,18] spectroscopy. The role of such silver clusters is, according to Shimizu *et al.*,[18] to act as sites for activation of molecular oxygen (formation of superoxide ions) with the aid of hydrogen. The superoxide ions subsequently partially oxidize the hydrocarbon, which in turn reacts with the NO_x species to form molecular nitrogen.[18] This is in line with Männikkö *et al.*,[5] who studied HC-SCR over 2 wt% Ag/Al_2O_3 and found carbon-containing reaction products of higher oxidation state in presence compared to absence of hydrogen. Recently, Yoshida *et al.*[20] demonstrated the presence of small silver clusters in a 5 wt% Ag/Al_2O_3 catalyst active for dehydrogenative coupling reactions, and it is likely that these silver species are similar to the ones active for the SCR reaction.

The strong promotional effect by hydrogen has also been shown for NH_3-SCR over the same type of catalyst.[21–24] Kondratenko *et al.*[22–23] performed thorough mechanistic studies of the NH_3-SCR reaction over a silver alumina catalyst with 1.7 wt% Ag loading. The authors conclude that the key-step for NH_3-SCR over this system is the dissociation of oxygen over reduced silver species, activating the ammonia. The authors suggest that these species are possibly larger silver particles of 3–5 nm, as resolved by high-resolution transmission electron microscopy (HRTEM) and UV-vis spectroscopy, or silver ions or clusters of a few atoms, indicated by UV-vis spectroscopy only, as the resolution of the microscope was not sufficient.[23] Especially considering the latter case (*i.e.* silver ions or clusters of a few atoms), the active site for NH_3-SCR suggested by Kondratenko *et al.*[23] appears to resemble the corresponding active site suggested for the HC-SCR reaction.[12,17–19] Previously, we have studied NO_x reduction with methanol over silver alumina samples

[a] *Competence Centre for Catalysis, Dept. Chemistry and Chemical Engineering, Chalmers University of Technology, SE-412 96 Göteborg, Sweden. E-mail: hanna.harelind@chalmers.se*
[b] *Laboratory of Industrial Chemistry and Chemical Engineering, Process Chemistry Centre, Åbo Akademi University, Biskopsgatan 8, FIN-20500 Turku/Åbo, Finland*
[c] *Competence Centre for Catalysis, Dept. Physics, Chalmers University of Technology, SE-412 96 Göteborg, Sweden*

This journal is © The Royal Society of Chemistry 2019

Catal. Sci. Technol., 2019, **9**, 6213–6216 | 6213

that show higher selectivity for N_2 formation when the large silver particles were leached out, leaving mainly small silver clusters and silver ions in the sample (as characterized by UV-vis spectroscopy, and TEM), compared to samples containing larger (nanometer-sized) silver particles.[16] The results showed that the selectivity towards N_2 formation is closely related to the types of silver species present in the sample with small clusters and ions favouring high selectivity for N_2 formation.

Here we study a 2 wt% silver alumina catalyst prepared† by a single-step sol–gel method including freeze-drying,[4] which is highly active for the SCR reaction with ammonia and hydrocarbons. The focus is to determine the size and state of the silver species in the sample. In Fig. 1 the characterization‡ results regarding catalytic activity and state of silver are presented. Fig. 1a shows the conversion of NO_x over temperature for the Ag/Al_2O_3 catalyst using ammonia or n-octane as reducing agent. With ammonia and in the presence of hydrogen, the catalyst is active (above 80% NO_x conversion) from below 150 to 550 °C, where the activity decreases due to oxidation of the reductant by molecular oxygen. For hydrogen assisted n-octane-SCR, the catalyst is active between 200 and 550 °C, in accordance with previous reports.[1] It can thus be concluded that the SCR performance of the catalyst prepared in the present study is well in line with previous studies and the catalyst can be considered as a representative sample. Fig. 1b shows the DRUV-vis (diffuse reflectance ultraviolet-visible) spectrum of the Ag/Al_2O_3 catalyst, with subtracted alumina background. By deconvolution of the absorption peaks it can be observed that the catalyst contains a relatively high amount of partially charged silver clusters ($Ag_n^{\delta+}$), indicated by the peaks centred at 300 and 360 nm,[18,25,26] and metallic silver (peaks above 390 nm), while the amount of ionic silver (230 nm (ref. 18, 25 and 26)) is relatively low, in agreement with previous reports.[18,25,26] In Fig. 1c, the results from the X-ray photoelectron spectroscopy (XPS) analysis of the oxidized (left) and reduced (right) 2 wt% silver alumina sample are shown. The Ag $3d_{5/2}$ peak shifts slightly towards lower binding energy (BE) when the sample is reduced, as compared to oxidized; 367.6 and 367.8 eV, respectively. This

is in line with previous studies[4] and the reason for this peculiar behaviour is a size effect of the silver particles: small silver clusters shift towards lower BE when reduced, in contrast to bulk silver.[27] Therefore, it can be concluded that silver clusters are present also on the silver alumina surface. Furthermore, no significant difference in the Ag $3d_{5/2}$ binding energy could be revealed after hydrothermal treatment (10% O_2, 10% H_2O at 500 °C, 12 h).[28] Hence, the silver species are stable.

Fig. 2 shows the fine-scale structure of the 2 wt% silver alumina sample using scanning transmission electron microscopy (STEM) with high-angle annular dark-field (HAADF) imaging.§ The imaging mode provides contrast from variations in atomic number and also from thickness variations. The imaging is combined with energy-dispersive X-ray spectroscopy (EDS) and electron energy loss spectroscopy (EELS) to determine the local elemental composition. Electron diffraction shows that the alumina is polycrystalline and the varying intensity of the alumina areas (Fig. 2) is due to the porous structure of the alumina. There are small areas of significantly higher intensity, which correspond to particles, few-atom clusters and individual atoms of silver. The insert in Fig. 2a shows the silver particle size distribution, with maximum at 2–3 nm. A cluster of five silver atoms can be observed in Fig. 2b and c. The configuration resembles theoretical predictions by first principles calculations for the shape of five-atom silver clusters, reported by Grönbeck et al.[29] Different cluster sizes with good correlations to the theoretical predictions are observed in the silver alumina sample. It should be noted that these few-atom clusters are not clearly visible in the HRTEM images. They also require correction of the spherical aberration of the condenser lens system (probe C_s correction) to be clearly distinguished in the STEM images. We are currently evaluating different approaches to statistically represent these individual atoms and few-atom clusters in particle size distributions. The implication of our data is that the common particle size distributions (see Fig. 2a) are not true representations since they do not show the small silver clusters (Fig. 2b and c). The HR-HAADF/STEM images clearly show the presence of atomically-resolved silver species, which
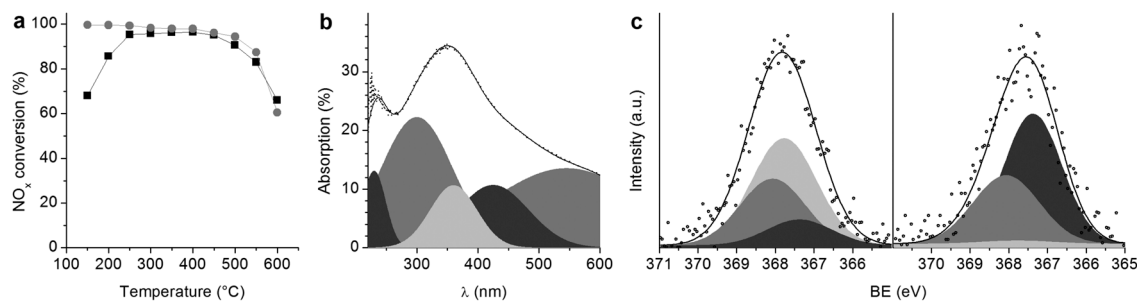

Fig. 1 Characterization‡ of the 2 wt% Ag/Al_2O_3 sample. a) H_2-assisted NO_x conversion over temperature, with NH_3 (grey circles) or n-octane (black squares) as reducing agent. b) Deconvoluted DRUV-vis spectrum, showing absorption peaks centred at 230, 300, 360, 425 and 545 nm. c) XPS spectra of the Ag $3d_{5/2}$ peak from oxidized (left) and reduced (right) sample. The deconvoluted peaks correspond to Ag (grey), Ag_2O (light grey) and AgO (dark grey).[32–35]
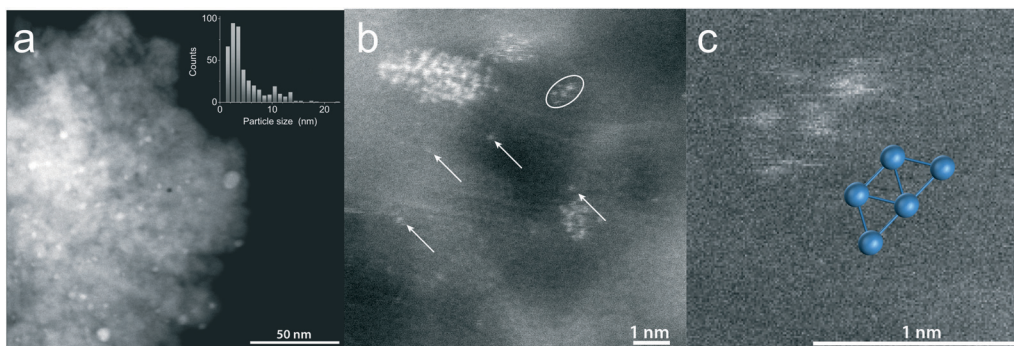
Fig. 2 HR-HAADF/STEM images of the Ag/Al$_2$O$_3$ sample. a) Overview and particle size distribution. b) Single silver atoms highlighted by arrows. A five-atom silver cluster is located within the ellipse. c) The cluster of five silver atoms is enhanced and compared to a ball-stick model as predicted by first principles calculations, according to Grönbeck et al.[29]

previously have been indicated by X-ray photoelectron and UV-vis spectroscopy for catalyst samples that are highly active for lean NO$_x$ reduction.

Conclusions

In this work, we show the first direct observations of individual silver atoms and few-atom clusters in silver alumina catalysts. The results support the previous suggestion of the presence of small silver clusters and strengthen the hypothesis of small silver clusters as active sites for selective catalytic reduction of nitrogen oxides. The configurations of the experimentally observed clusters correlate with the theoretical predictions.[29] This is an important step towards the understanding of the catalytic processes that occur in silver alumina catalysts active for the selective reduction of nitrogen oxides.

Conflicts of interest

There are no conflicts to declare.

Acknowledgements

Notes and references

† Sample synthesis. The Ag/Al$_2$O$_3$ catalyst and the alumina reference sample were prepared according to the sol–gel method combined with freeze-drying, as described by Kannisto et al.[4] Silver nitrate (>99.5%; VWR) was dissolved in Milli-Q water (18 MΩ cm) and aluminum isopropoxide (98+%; Aldrich) was slowly added to the AgNO$_3$ solution under vigorous stirring. The resulting slurry was heated to 80 °C and nitric acid (10%; Fluka) was subsequently drop-wise

added until a sol was formed. The sol was then kept under stirring for 12 h. Excess solvent was removed under reduced pressure at 30 °C until a gel was formed. The gel was thereafter instantly frozen with liquid nitrogen, freeze-dried, heated in air from room temperature (RT) at 2 °C min^{-1} to 600 °C and finally calcined at this temperature for 6 h.

‡ Sample characterization. The NO$_x$ conversion was investigated in flow reactor experiments over Ag/Al$_2$O$_3$ grains (0.4 g, diameter distribution 250–500 μm) according to the same procedure as described by Arve et al.[30] The total flow was 550 ml min^{-1} at RT, corresponding to a gas hourly space velocity (GHSV) of 60 000 h^{-1}. A temperature range of 150–600 °C with sampling at steady-state conditions (30 min for every 50 °C) was used for the flow reactor experiments. The gas mixture used in the experiments consisted of 500 vol. ppm NO, 1 vol% H$_2$, 6 vol% O$_2$, 10 vol% CO$_2$, 350 vol. ppm CO, 12 vol% H$_2$O, and He as balance. The reducing agents used were n-octane (375 vol. ppm, C/N = 6), or ammonia (500 vol. ppm, NO/NH$_3$ = 1). N$_2$-physisorption was performed at 77 K using a Micromeritics Tristar instrument. The specific surface area and the pore size distribution of the prepared Ag/Al$_2$O$_3$ and pure Al$_2$O$_3$ samples were determined according to the BET and BJH method, respectively. The samples were dried at 200 °C in vacuum for 2 h before the analysis. The surface area of the 2 wt% Ag/Al$_2$O$_3$ sample was 187 m^2 g^{-1}, and the average pore size (BJH adsorption–desorption) was 36–43 nm. The corresponding values for the alumina sample were 192 m^2 g^{-1}, and 41–47 nm, respectively. DRUV-vis spectra were collected using a Cary 5000 UV-vis-NIR spectrophotometer equipped with an External DRA-2500. The integrating sphere permitted fast acquisition of high-quality (high-resolution, low-noise) spectra. The spectra were recorded in the 200–1500 nm wavelength range, using the appropriate baseline correction. The spectrum from the alumina sample was used as background. XPS measurements were performed to determine the oxidation state of silver in the Ag/Al$_2$O$_3$ sample. The measurements were performed using a Perkin-Elmer PHI 5000 C system, equipped with a pre-treatment reactor cell, as described previously by Olsson and Fridell.[31] Pre-treatment was performed for 20 min at 400 °C, in a gas flow of either 2 vol% O$_2$ or 2 vol% H$_2$ (50 ml min^{-1}, Ar bal.). The sample was then cooled in an argon flow, before being transferred to the UHV chamber. XPS spectra were obtained using a monochromated Al K$_\alpha$ X-ray source. Charging of the sample was accounted for by shifting the spectrum against the C 1s peak at 284.5 eV.[32]

§ Scanning transmission electron microscopy. HAADF/STEM imaging for particle size determination was performed using a FEI Titan 80–300 TEM, with a corrector of spherical aberration (C$_s$) of the condenser lens system. The microscopy data was recorded at 300 kV. Elemental analysis was carried out using EDS and EELS. The samples were prepared by thoroughly crushing the powder catalyst in a mortar and subsequently mixing the sample with ethanol. A drop of the resulting mix was then placed on a carbon sputtered copper grid (3.0 mm, 300 mesh).

1 R. Burch, *Catal. Rev.: Sci. Eng.*, 2004, **46**, 271.

2 T. Miyadera, *Appl. Catal., B*, 1993, **2**, 199.

This journal is © The Royal Society of Chemistry 2019

Catal. Sci. Technol., 2019, **9**, 6213–6216 | **6215**

3   H. Kannisto, K. Arve, T. Pingel, A. Hellman, H. Härelind, K. Eränen, E. Olsson, M. Skoglundh and D. Y. Murzin, *Catal. Sci. Technol.*, 2013, **3**, 644.

4   H. Kannisto, H. H. Ingelsten and M. Skoglundh, *J. Mol. Catal. A: Chem.*, 2009, **302**, 86.

5   M. Männikkö, M. Skoglundh and H. H. Ingelsten, *Appl. Catal., B*, 2012, **119–120**, 256.

6   F. Gunnarsson, J. Pihl, T. Toops, M. Skoglundh and H. Härelind, *Appl. Catal., B*, 2017, **202**, 42.

7   F. Gunnarsson, M. Z. Granlund, M. Englund, J. Dawody, L. J. Pettersson and H. Härelind, *Appl. Catal., B*, 2015, **162**, 583.

8   C. J. Niu, J. H. Niu, S. M. Wang, Z. W. Wang, S. Y. Dong, H. Y. Fan, Y. Hong and D. P. Liu, *Catal. Commun.*, 2019, **123**, 49.

9   G. Y. Xu, Y. B. Yu and H. He, *J. Phys. Chem. C*, 2018, **122**, 670.

10 M. Barreau, M.-L. Tarot, D. Duprez, X. Courtois and F. Can, *Appl. Catal., B*, 2018, **220**, 19.

11 S. Satokawa, *Chem. Lett.*, 2000, **29**, 294.

12 J. P. Breen and R. Burch, *Top. Catal.*, 2006, **39**, 53.

13 M. M. Azis, H. Härelind and D. Creaser, *Chem. Eng. J.*, 2013, **221**, 382.

14 M. M. Azis, H. Härelind and D. Creaser, *Catal. Sci. Technol.*, 2015, **5**(1), 296.

15 M. Männikkö, M. Skoglundh and H. Härelind, *Top. Catal.*, 2015, **58**(14), 977.

16 M. Männikkö, X. Wang, M. Skoglundh and H. Härelind, *Appl. Catal., B*, 2016, **180**, 291.

17 J. P. Breen, R. Burch, C. Hardacre and C. J. Hill, *J. Phys. Chem. B*, 2005, **109**, 4805.

18 K. Shimizu, M. Tsuzuki, K. Kato, S. Yokota, K. Okumura and A. Satsuma, *J. Phys. Chem. C*, 2007, **111**, 950.

19 J. Shibata, Y. Takada, A. Shichi, S. Satokawa, A. Satsuma and T. Hattori, *J. Catal.*, 2004, **222**, 368.

20 K. Yoshida, K. Kon and K. Shimizu, *Top. Catal.*, 2016, **59**, 1740.

21 M. Richter, R. Fricke and R. Eckelt, *Catal. Lett.*, 2004, **94**, 115.

22 E. V. Kondratenko, V. A. Kondratenko, M. Richter and R. Fricke, *J. Catal.*, 2006, **239**, 23.

23 V. A. Kondratenko, U. Bentrup, M. Richter, T. W. Hansen and E. V. Kondratenko, *Appl. Catal., B*, 2008, **84**, 497.

24 D. E. Doronkin, S. Fogel, S. Tamm, L. Olsson, T. S. Khan, T. Bligaard, P. Gabrielsson and S. Dahl, *Appl. Catal., B*, 2012, **113–114**, 228.

25 N. Bogdanchikova, F. C. Meunier, M. Avalos-Borja, J. P. Breen and A. Pestryakov, *Appl. Catal., B*, 2002, **36**, 287.

26 A. N. Pestryakov and A. A. Davydov, *J. Electron Spectrosc. Relat. Phenom.*, 1995, **74**, 195.

27 D. Guo, Q. Guo, K. Zheng, E. G. Wang and X. Bao, *J. Phys. Chem. C*, 2007, **111**, 3981.

28 F. Gunnarsson, J.-Y. Zheng, H. Kannisto, C. Cid, A. Lindholm, M. Milh, M. Skoglundh and H. Härelind, *Top. Catal.*, 2013, **56**, 416.

29 H. Grönbeck, A. Hellman and A. Gavrin, *J. Phys. Chem. A*, 2007, **111**, 6062.

30 K. Arve, L. Capek, F. Klingstedt, K. Eränen, L. E. Lindfors, D. Y. Murzin, J. Dedecek, Z. Sobalik and B. Wichterlova, *Top. Catal.*, 2004, **30–31**, 91.

31 L. Olsson and E. Fridell, *J. Catal.*, 2002, **210**, 340.

32 J. F. Moulder, W. F. Stickle, P. E. Sobol and K. D. Bomben, *Handbook of X-ray photoelectron spectroscopy*, Perkin-Elmer Corporation - Physical Electronics Division, Eden Prairie, 1992.

33 G. Schön, *Acta Chem. Scand.*, 1973, **27**, 2623.

34 M. Bielmann, P. Schwaller, P. Ruffieux, O. Groning, L. Schlapbach and P. Groning, *Phys. Rev. B: Condens. Matter Mater. Phys.*, 2002, **65**, 235431.

35 J. F. Weaver and G. B. Hoflund, *J. Phys. Chem.*, 1994, **98**, 8519.

6216 | *Catal. Sci. Technol.*, 2019, **9**, 6213–6216

This journal is © The Royal Society of Chemistry 2019